

Optimal Implementations for Reliable Circadian Clocks

Yoshihiko Hasegawa^{1*} and Masanori Arita^{2,3}

¹*Department of Biophysics and Biochemistry, Graduate School of Science,
The University of Tokyo, Tokyo 113-0033, Japan;*

²*Center for Information Biology, National Institute of Genetics, Shizuoka 411-8540, Japan; and*

³*RIKEN Center for Sustainable Resource Science, Kanagawa 230-0045, Japan.*

Circadian rhythms are acquired through evolution to increase the chances for survival through synchronizing with the daylight cycle. Reliable synchronization is realized through two trade-off properties: regularity to keep time precisely, and entrainability to synchronize the internal time with daylight. We found by using a phase model with multiple inputs that achieving the maximal limit of regularity and entrainability entails many inherent features of the circadian mechanism. At the molecular level, we demonstrate the role sharing of two light inputs, phase advance and delay, as is well observed in mammals. At the behavioral level, the optimal phase-response curve inevitably contains a dead zone, a time during which light pulses neither advance nor delay the clock. We reproduce the results of phase-controlling experiments entrained by two types of periodic light pulses. Our results indicate that circadian clocks are designed optimally for reliable clockwork through evolution.

PACS numbers: 87.18.Yt, 87.18.Tt, 05.45.Xt

Many terrestrial species, from cyanobacteria through to humans, adapt to sunlight and have acquired circadian oscillatory systems. Although their molecular implementation is species dependent [1], all exhibit a regular rhythm of 24-h that can be entrained by light input. Two fundamental properties are necessary for circadian clocks [2], i.e. *regularity* to keep time precisely [3–5] and *entrainability* to adjust the internal time through light stimuli [6–8]. It is not easy to maximize entrainability and regularity simultaneously; higher entrainability implies more vulnerability to noise, whereas higher regularity signifies less flexibility to entrainment. We studied an optimal phase-response curve (PRC) problem for a one-input pathway in [9]. In the present Letter, we generalize the calculations of [9] and formalize the optimal implementation problem for multiple input pathways without relying on specific oscillator models [7, 10, 11]. We show that the simultaneous maximization of entrainability and regularity entails several inherent properties of circadian clocks. At the molecular level, we rationalize the role sharing of multiple input pathways which was reported in murine circadian clocks [12, 13]. At the behavioral level, we rationalize a time period during which the time is neither advanced nor delayed by light in an optimal clock [14]. Our theory can also explain different gene expression patterns when entrained by two different light pulses [15]. In this study we investigate the optimal implementations for multiple input pathways to achieve maximal limit of entrainability and regularity. Although all circadian clocks transmit light signals through multiple pathways [7, 10, 11], entrainment problems in multiple pathways have been little studied.

Circadian clocks keep time regularly under molecular noise [3–5]. It is also entrainable by periodic light stimuli. To consider these effects, we use an N -

dimensional Langevin equation with respect to x_i , which is the concentration of i th molecular species: $\dot{x}_i = F_i(\mathbf{x}; \rho) + Q_i(\mathbf{x})\xi_i(t)$ where $F_i(\mathbf{x}; \rho)$ is the i th reaction rate ($i = 1, 2, \dots, N$), $Q_i(\mathbf{x})$ is a multiplicative noise term, and $\xi_i(t)$ is white Gaussian noise with $\langle \xi_i(t)\xi_j(t') \rangle = 2\delta_{ij}\delta(t-t')$. To incorporate the effect of light, we introduce a light-sensitive parameter ρ which is perturbed as $\rho \rightarrow \rho + d\rho$ when stimulated by light. We quantify regularity by the temporal variance in the oscillation. From [9], the period variance is known to be $\mathcal{V}_T \simeq T^3(4\pi^3)^{-1} \int_0^{2\pi} \sum_{i=1}^N U_i(\theta)^2 Q_i(\theta)^2 d\theta$, where T is the period of the unperturbed oscillator, $\mathbf{U}(\phi) = (U_1(\phi), \dots, U_N(\phi))$ is the infinitesimal PRC (iPRC) defined by $\mathbf{U}(\phi) = \nabla_{\mathbf{x}}\phi|_{\mathbf{x}=\mathbf{x}_{\text{LC}}(\phi)}$ and $\mathbf{x}_{\text{LC}}(\phi)$ is a point on the limit-cycle trajectory at phase $\phi \in [0, 2\pi)$. Entrainability is quantified as the width of the Arnold tongue. The phase dynamics with periodic input signals are described by a tilted periodic potential. If stable points exist in the potential, the oscillator can be entrained by input signals [16]. Thus we can discuss entrainability without considering noise because the existence of stable points does not depend on noise. Therefore we set $Q_i(\mathbf{x}) = 0$. Let $p(\omega t)$ be an input signal with angular frequency ω . For a weak input signal $d\rho = \chi p(\omega t)$ ($\chi \geq 0$ is the signal strength), we obtain $\dot{\phi} = \Omega + \chi Z(\phi)p(\omega t)$ ($\phi \in [0, 2\pi)$ is the phase and $\Omega = 2\pi/T$) where

$$Z(\phi) = \sum_{i=1}^N Z_i(\phi), \quad Z_i(\phi) = \frac{\partial F_i(\phi; \rho)}{\partial \rho} U_i(\phi), \quad (1)$$

with $F_i(\phi; \rho) = F_i(\mathbf{x}_{\text{LC}}(\phi); \rho)$. $Z_i(\phi)$ quantifies phase shift due to the perturbation of ρ in the i th coordinate. We hereafter refer to $Z(\phi)$ as the *parametric PRC* (pPRC) [9, 17]. The dynamics of a slow variable defined

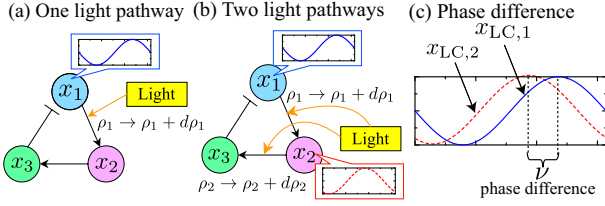


FIG. 1: Examples of (a) one-light input pathway and (b) two-light input pathway cases. The insets describe the time course of molecular species that are affected by light stimuli. In (b) the light-sensitive molecular species correspond to x_1 and x_2 that exhibit peaks at different phase (this difference is given by ν). (c) The phase difference ν is defined by the difference between k_1 th and k_2 th molecular species.

by $\psi = \phi - \omega t$ obeys

$$\dot{\psi} = \Omega - \omega + \chi \Theta(\psi), \quad (2)$$

where $\Theta(\psi) = (2\pi)^{-1} \int_0^{2\pi} Z(\psi + \theta) p(\theta) d\theta$. The width of the Arnold tongue is given by $\chi \mathcal{E}$, where $\mathcal{E} = (2\pi)^{-1} \int_0^{2\pi} Z(\theta) \{p(\theta - \psi_M) - p(\theta - \psi_m)\} d\theta$ with $\psi_M = \text{argmax}_\psi \Theta(\psi)$ and $\psi_m = \text{argmin}_\psi \Theta(\psi)$ [9, 18]. Optimal circadian clocks are derived as optimal PRCs $U_i(\phi)$ which were obtained with the variational method by maximizing the entrainability \mathcal{E} subject to constant variance $\mathcal{V}_T = \sigma_T^2$: $U_i(\phi) = \pi^2 T^{-3} \lambda^{-1} Q_i(\phi)^{-2} \{p(\phi - \psi_M) - p(\phi - \psi_m)\} \partial_\rho F_i(\phi; \rho)$ (λ is a Lagrange multiplier [19]) [9].

We generalize the above scheme to multiple input signals. Suppose there are M input pathways and parameters $\rho_1, \rho_2, \dots, \rho_M$ are affected as $\rho_i \rightarrow \rho_i + d\rho_i$ under light stimuli. By introducing an auxiliary scaling parameter s_i defined by $d\rho_i = s_i d\rho$, each parameter perturbation is reparameterized as

$$\rho_i \rightarrow \rho_i + d\rho_i \Rightarrow \tilde{\rho}_i + s_i \rho \rightarrow \tilde{\rho}_i + s_i(\rho + d\rho), \quad (3)$$

where $\tilde{\rho}_i = \rho_i - s_i \rho$. Through this reparameterization, the multiple perturbations can be reduced to a single parameter case with respect to ρ . In this instance, ρ in Eq. (3) is a hypothetical parameter and has no correspondence to actual reaction rates.

Light stimuli generally affect the rate constants, but the detailed mechanisms vary between organisms [21]. Our model can cover these different entrainment mechanisms. We first explain a simple case (Fig. 1(a)), and then generalize it. In Fig. 1(a), we assume that light stimuli enhance the synthesis rate of x_2 , where the dynamics of x_2 can be described by $\dot{x}_2 = \rho_{\text{syn}} x_1 + \rho_{\text{deg}} x_2$ where $\rho_{\text{syn}} > 0$ and $\rho_{\text{deg}} < 0$ are the synthesis and degradation rates, respectively. Because the synthesis rate increases when stimulated by light, by taking $\rho = \rho_{\text{syn}}$ (ρ is the light-sensitive parameter), the rate equation can be divided into ρ -dependent and ρ -independent parts $\dot{x}_2 = F_2(\mathbf{x}; \rho) = \rho_{\text{deg}} x_2 + \rho x_1 = \tilde{F}_2(\mathbf{x}) + \rho x_1$, where $\tilde{F}_2(\mathbf{x})$

denotes terms not including ρ in $F_2(\mathbf{x}; \rho)$. We next consider a generic case with two-input pathways ($M = 2$). Let us assume that light stimuli affect parameters ρ_1 and ρ_2 (e.g. translation, transcription or degradation rate) which depend on k_1 th and k_2 th molecular species and affect j_1 th and j_2 th species, respectively (e.g. $k_1 = 1$, $k_2 = 2$, $j_1 = 2$ and $j_2 = 3$ in Fig. 1(b)). The rate equations $F_{j_i}(\mathbf{x}; \rho)$ of j_1 th and j_2 th are described as

$$\dot{x}_{j_i} = \tilde{F}_{j_i}(\mathbf{x}) + \rho_i x_{k_i} = \underbrace{\tilde{F}_{j_i}(\mathbf{x})}_{\rho\text{-independent}} + \underbrace{\tilde{\rho}_i x_{k_i}}_{\rho\text{-dependent}}, \quad (4)$$

where $i = 1, 2$ and $\tilde{F}_{j_i}(\mathbf{x})$ denotes terms not including ρ_i in $F_{j_i}(\mathbf{x}; \rho)$. From Eq. (1), we see that PRCs are only concerned with the derivative of $F_{j_i}(\mathbf{x}; \rho)$ with respect to ρ , which is specifically given by $\partial_\rho F_{j_i}(\mathbf{x}; \rho) = s_i x_{k_i}$. Consequently, the ρ -independent part in Eq. (4) plays no role in the formation of optimal PRCs. We approximate x_k by the k th coordinate of \mathbf{x}_{LC} , denoted as $x_{\text{LC},k}(\phi)$ in Eq. (4). Because $x_{\text{LC},k}(\phi)$ oscillates, we model it with a sine curve. k_1 th and k_2 th molecular species may peak at different times as shown in Fig. 1(b), where the time courses of the k_1 th and k_2 th molecular species is described in the insets by solid and dashed lines, respectively. Therefore, the time course is approximated by $x_{\text{LC},k_i}(\phi) = 1 - \alpha_i \sin(\phi + u_{k_i})$ for $i = 1, 2$, where u_{k_1} and u_{k_2} are initial phases of k_1 th and k_2 th molecular species, the amplitude α_i being assumed as identical $\alpha_1 = \alpha_2 = \alpha$ ($0 \leq \alpha \leq 1$). Let ν be the phase difference between k_1 th and k_2 th molecular species, i.e. $\nu = u_{k_2} - u_{k_1}$ (Fig. 1(c)). This parameter plays an important role in optimization.

Circadian clocks are entrained by sunlight whose intensity is determined by 24-h periodic solar irradiance. The solar irradiance I with respect to the zenith angle ϑ is given by $I = I_0 \cos \vartheta$, where I_0 is the irradiance at $\vartheta = 0$, and I vanishes when the sun is below the horizon [22]. Thus we approximate its time course by $p(\omega t) = \sin(\omega t)$ for $0 \leq \text{mod}(\omega t, 2\pi) < \pi$ (day) and $p(\omega t) = 0$ for $\pi \leq \text{mod}(\omega t, 2\pi) < 2\pi$ (night) with $\text{mod}(x, y) = x \text{ mod } y$, which we call *solar radiation input* [9].

Our model starts from the two-input case ($M = 2$). The noise term was introduced only for input molecules ($Q_{j_1}(\phi) = \sqrt{q}$, $Q_{j_2}(\phi) = \sqrt{q}$ and $Q_i(\phi) = 0$ otherwise, where q is the noise intensity), and we set $u_{k_1} = 0$ (i.e. $\nu = u_{k_2}$), $T = 1$, $\sigma_T^2 = 1$, and $q = 1$ without loss of generality. We then need to specify additional parameters s_1 and s_2 (Eq. (3)) that determine the strength of the input signal relative to ρ . If we are concerned with pPRCs (experimentally observed PRCs) only, the sign of s_i (positive or negative) does not play any role, because s_i is squared in the optimal pPRCs. We set $s_1 = s_2 = 1$ for simplicity; this corresponds to assuming equal weight for each light input pathway.

Figure 2(a) shows the ν dependence of maximal entrainability for $\alpha = 0.5$ (solid line) and $\alpha = 1$ (dashed

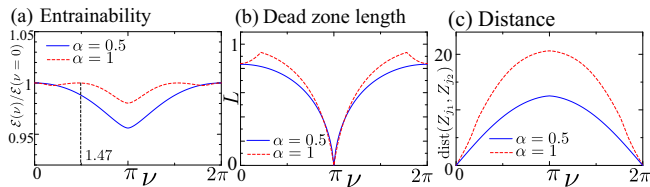


FIG. 2: (a) Normalized entrainability as a function of ν for $\alpha = 0.5$ (solid line) and $\alpha = 1$ (dashed line). The value is normalized by the entrainability at $\nu = 0$ (i.e. $\mathcal{E}(\nu)/\mathcal{E}(\nu = 0)$). For $\alpha = 1$, maximal is achieved at $\nu = 0$ and 1.47 . (b) Dead zone length L as a function of the phase difference ν for $\alpha = 0.5$ (solid line) and $\alpha = 1$ (dashed line). (c) Distance between $Z_{j_1}(\phi)$ and $Z_{j_2}(\phi)$ as a function of ν for $\alpha = 0.5$ (solid line) and $\alpha = 1$ (dashed line).

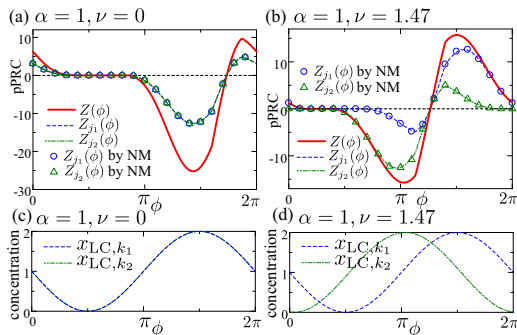


FIG. 3: (a)–(b) Optimal PRCs ($Z(\phi)$, $Z_{j_1}(\phi)$, and $Z_{j_2}(\phi)$) for (a) $\alpha = 1$ and $\nu = 0$ and (b) $\alpha = 1$ and $\nu = 1.47$. In (a) and (b), $Z(\phi)$, $Z_{j_1}(\phi)$ and $Z_{j_2}(\phi)$ obtained with the variational method, are plotted with thick solid lines, dashed lines and dot-dash lines, respectively. $Z_{j_1}(\phi)$ and $Z_{j_2}(\phi)$ obtained with a numerical method (NM) are plotted with circles and triangles, respectively [19]. In (a), PRCs that are symmetric with respect to the horizontal axis or $\phi = 3\pi/2$ are also optimal. In (b), PRCs that are symmetric with respect to the horizontal axis are also optimal. (c)–(d) Time course of the molecular species concentration for (c) $\alpha = 1$ and $\nu = 0$ and (d) $\alpha = 1$ and $\nu = 1.47$. Two species x_{LC,k_1} and x_{LC,k_2} are plotted with dashed and dot-dash lines. In (a) and (c), dashed and dot-dashed lines are indistinguishable.

line). For $\alpha = 0.5$, the maximum was achieved at $\nu = 0$ where no phase difference existed. However, upon increasing α to 1, maximal entrainability was achieved at two points, $\nu = 0$ and $\nu = 1.47$ (Figs. 3(a) and (b)). Interestingly, optimality can be attained in the presence of phase difference. From Eq. (1), we divide the pPRC $Z(\phi)$ into contributions from two input pathways $Z(\phi) = Z_{j_1}(\phi) + Z_{j_2}(\phi)$, where $Z_{j_1}(\phi)$ and $Z_{j_2}(\phi)$ quantify the phase shift produced by the 1st and 2nd input pathways, respectively. Optimal $Z(\phi)$, $Z_{j_1}(\phi)$, and $Z_{j_2}(\phi)$ for the two-input case are plotted in Figs. 3(a) and (b). Figures 3(c) and (d) are the corresponding time course of the k_1 th and k_2 th molecular species concentration. We see that optimal PRCs $Z(\phi)$ in Figs. 3(a) and (b) are very similar to experimentally observed PRCs in

which there is a dead zone, a time during which light neither advanced nor delayed the clock ($1 \lesssim \phi \lesssim 2$ in Figs. 3(a) and (b)). Intriguingly, experimental studies in different species reported the existence of the dead zone [14]. Although cases with $\nu = 0$ and $\nu = 1.47$ achieved the same entrainability, $Z(\phi)$ for $\nu = 0$ is asymmetric with respect to horizontal axis, which entails an asymmetric Arnold tongue. Thus for a symmetric Arnold tongue, only $\nu = 1.47$ can achieve maximal entrainability. We calculated the ν dependence of the dead zone length L (length of null parts in PRCs [19]) in Fig. 2(b) for $\alpha = 0.5$ (solid line) and $\alpha = 1.0$ (dashed line). In Fig. 2(b), L quickly diminishes around $\nu = \pi$, showing that a dead zone always appears in optimal PRCs except for a singular point $\nu = \pi$.

The fundamental difference of $\nu = 1.47$ from $\nu = 0$ is the role sharing of two PRCs Z_{j_1} and Z_{j_2} (Fig. 3(b)). Z_{j_1} is responsible for the phase advance and Z_{j_2} for the delay (the positive part of Z_{j_1} is larger than the negative part and vice versa). This effect was observed for all ν values except $\nu = 0$, as shown below. We quantify the distance between Z_{j_1} and Z_{j_2} by $\text{dist}(Z_{j_1}, Z_{j_2}) = \sqrt{\int_0^{2\pi} \{Z_{j_1}(\theta) - Z_{j_2}(\theta)\}^2 d\theta}$, which becomes larger when the two PRCs play more compensatory roles. The distance calculated as a function of ν for $\alpha = 0.5$ (solid line) and $\alpha = 1$ (dashed line) is shown in Fig. 2(c) where the distance is maximal exactly at $\nu = \pi$. When a phase difference ($\nu > 0$) exists, this role-sharing between two-input pathways always yields a synchronization advantage. There is experimental evidence for advance and delay roles of *Per1* and *Per2*, respectively, in mice [12]. In this regard, Ref. [13] observed a period dependence of *Per1* and *Per2* knockout mutants on the intensity of constant light. We can reproduce this result with optimal PRCs as follows. Note that entrainability is maximal at $\nu = 1.47$ for $\alpha = 1$ (Fig. 3(b)). Consequently, we set the clock parameters to $\alpha = 1$ and $\nu = 1.47$. Under a constant light condition, the input signal is modeled by $dp = \chi p(t)$, where $p(t) = 1$. By integrating the phase equation $\dot{\phi} = \Omega + \chi Z(\phi)p(t)$ from $t = 0$ to $t = T$ where $\phi(t = 0) = 0$, the phase at time T with input strength χ is given by $\phi(T; \chi) = 2\pi + (2\pi)^{-1} T \chi \int_0^{2\pi} Z(\theta) d\theta$. For weak χ , the period T_χ , which is the period under a constant light condition, is approximated by $T_\chi/T \simeq \phi(T; 0)/\phi(T; \chi) \simeq 1 - T\chi(4\pi^2)^{-1} \int_0^{2\pi} Z(\theta) d\theta$ [17, 19]. Assuming $x_{j_1} = [\textit{Per1}]$ and $x_{j_2} = [\textit{Per2}]$, we simulated *Per1* and *Per2* mutants by setting $Z(\phi) = Z_{j_2}(\phi)$ and $Z(\phi) = Z_{j_1}(\phi)$, respectively. When increasing the intensity χ of constant light, the period ratio T_χ/T increases for *Per1* mutant and decreases for *Per2* mutant. This result agrees with the experimental evidence (Fig. 2 in [13]).

Our model can further suggest insights into the molecular mechanism of the clock. In hamsters, Schwartz *et al.* [15] reported different gene expressions of *Per1* and

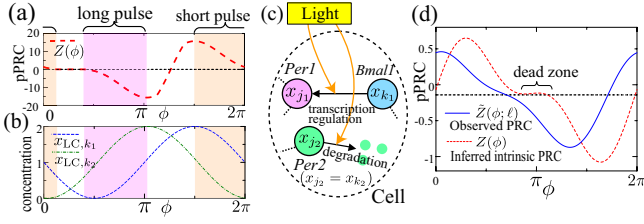


FIG. 4: (a)–(c) Theoretical reproduction of a light entrainment experiment involving hamsters [15]. (a) Optimal pPRC $Z(\phi)$ of the two-input case $M = 2$ with $\alpha = 1$ and $\nu = 1.47$ (Fig. 3(b)). (b) The time course of the molecular species concentration of x_{LC,k_1} (dashed lines) and x_{LC,k_2} (dot-dash lines) for $\alpha = 1$ and $\nu = 1.47$. (c) Molecular implementation of the murine light entrainment mechanism. The model can be described by Eq. (4) with $x_{j_1} = [Per1]$, $x_{k_1} = [Bmal1]$, and $x_{j_2} = x_{k_2} = [Per2]$. (d) Observed (solid line) and inferred-intrinsic ($N_\mu = 2$, $\chi = 1$; dashed line) pPRCs of humans as a function of the onset of pulses. Observed pPRC is brought from Ref. [23], which measured pPRC with $\ell = 6.7$ -h light pulses. The horizontal dashed line indicates anticipated phase delay [23].

Per2 when entrained by two types of periodic light pulses that have short (23.33-h) and long (24.67-h) periods. Let us reproduce Schwartz’s experiment in our optimization framework with two inputs. We again set $\alpha = 1$ and $\nu = 1.47$ and assume $x_{j_1} = [Per1]$ and $x_{j_2} = [Per2]$. Ref. [15] applied a periodic light pulse of 1-h duration, which we modeled with a periodic δ -function

$$p(\omega t) = 2\pi\delta(\text{mod}(\omega t, 2\pi)), \quad (5)$$

where a factor 2π ensures $\Theta(\psi) = (2\pi)^{-1} \int_0^{2\pi} p(\theta - \psi)Z(\theta)d\theta = Z(\psi)$. Given the periodic light pulse (Eq. (5)), the entrainment phase ψ_{st} (i.e. the circadian time at which hamsters receive the light pulses) can be determined by

$$\Omega - \omega + \chi\Theta(\psi_{st}) = 0, \quad \Theta'(\psi_{st}) < 0, \quad (6)$$

where we used Eq. (2). Thus ψ_{st} can be given as a solution of $Z(\psi_{st}) = (\omega - \Omega)/\chi$ with $Z'(\psi_{st}) < 0$. For the long ($\omega < \Omega$) and short ($\omega > \Omega$) pulses, $(\omega - \Omega)/\chi$ becomes negative and positive, respectively. This shows that the long and short pulses always act on hamsters at early ($\phi = 1.3 \sim 3.2$; purple in Figs. 4(a) and (b)) and late ($\phi = 4.7 \sim 0.47$; orange in Figs. 4(a) and (b)) subjective night, respectively. The effects of the light pulse on the circadian clock depend on the concentration of x_{k_1} and x_{k_2} at these phases (Eq. (4)). For the long pulse, we obtain $x_{LC,k_1} < x_{LC,k_2}$ (Fig. 4(b)), which indicates that the long pulse always affects the expression of x_{j_2} whereas it influences x_{j_1} only a little. In contrast, the short pulse affects x_{j_1} more strongly than x_{j_2} . Our result shows that, provided the circadian clocks are designed optimally, long and short pulses affect the expression of two different components (*Per2* and *Per1*) differently. Surprisingly,

our expression patterns agree with the experiments of Schwartz *et al.* [15]. They hypothesized that light stimuli affect the transcription of *Per1* and the degradation of *Per2*. In their molecular terms, k_1 th and k_2 th species in our framework correspond to *Bmal1* and *Per2*, which regulate the light effect (transcription and degradation) on *Per1* and *Per2*, respectively (i.e. $x_{k_1} = [Bmal1]$ and $x_{k_2} = [Per2]$). Figure 4(c)). The phase difference between *Per2* and *Bmal1* was experimentally determined as $\nu \sim 2$ [24] and close to our result ($\nu = 1.47$).

The pPRCs hitherto discussed are *intrinsic* in the sense that they represent the internal clock dynamics. The intrinsic pPRCs can be observed only through the phase shift induced by short light pulses [14]. Theoretically, precise measurement is possible only through δ -peaked stimuli. In experiments involving higher organisms, however, light pulses are much longer than the δ -peaked function, and observed pPRCs become different from the intrinsic ones. To study the relation between intrinsic and observed pPRCs, let us consider a squared-pulse stimulation $d\rho = \chi p(t)$ with $p(t) = \ell^{-1}H(t - t_s)H(\ell + t_s - t)$ where $H(t)$ is the Heaviside step function, t_s is onset time of the pulses and ℓ is the pulse duration. For $\ell \rightarrow 0$, the squared pulse reduces to a δ -function $\delta(t - t_s)$. Let $\tilde{Z}(\phi; \ell)$ be an observed pPRC of $Z(\phi)$ by a light pulse with the duration ℓ . Observed and intrinsic pPRCs can be related via $c_\mu = -i\tilde{c}_\mu\ell\mu\Omega/\{\chi(1 - \exp(i\mu\Omega\ell))\}$ for $\mu \neq 0$ and $c_\mu = \tilde{c}_\mu/\chi$ for $\mu = 0$, where c_μ and \tilde{c}_μ are Fourier coefficients of intrinsic and observed pPRCs, respectively ($Z(\phi) = \sum_{\mu=-N_\mu}^{N_\mu} c_\mu \exp(i\mu\phi)$ and $\tilde{Z}(\phi; \ell) = \sum_{\mu=-N_\mu}^{N_\mu} \tilde{c}_\mu \exp(i\mu\phi)$ with N_μ being an expansion order). By this method, we inferred the intrinsic pPRC from an observed pPRC in human [23] ($\ell = 6.7$ -h) where a dead zone is seemingly nonexistent [19]. The inferred pPRC (dashed line) and the observed pPRC (solid line) are shown in Fig. 4(d), where the phase (horizontal axis) represents the onset of the pulse. This result suggests that superficial pPRCs may lack a dead zone even though their innate mechanisms actually do.

We have demonstrated that key properties of circadian clocks are consequences of optimization to attain the maximal limit of entrainability and regularity. Our theory explains known experimental results such as the role sharing of two inputs and different gene expression patterns by different pulses. We also explain the superficial absence of a dead zone in human. The model can be used to reveal key molecular elements responsible for the clock.

This work was supported by Grant-in-Aid for Young Scientists B (Y.H.: No. 25870171) and for Innovative Areas “Biosynthetic machinery” (M.A.) from MEXT, Japan.

-
- * Corresponding author: yoshihiko.hasegawa@gmail.com;
Present address: Department of Information and Communication Engineering, Graduate School of Information Science and Technology, The University of Tokyo, Tokyo 113-8656, Japan
- [1] M. W. Young and S. A. Kay, *Nat. Rev. Genet.* **2**, 702 (2001).
 - [2] C. H. Johnson, P. L. Stewart, and M. Egli, *Annu. Rev. Biophys.* **40**, 143 (2011).
 - [3] J. M. G. Vilar, H. Y. Kueh, N. Barkai, and S. Leibler, *PNAS* **99**, 5988 (2002).
 - [4] D. Gonze, J. Halloy, and A. Goldbeter, *PNAS* **99**, 673 (2002).
 - [5] E. D. Herzog, S. J. Aton, R. Numano, Y. Sakaki, and H. Tei, *J. Biol. Rhythms* **19**, 35 (2004).
 - [6] D. Gonze and A. Goldbeter, *J. Stat. Phys.* **101**, 649 (2000).
 - [7] T. Roenneberg, S. Daan, and M. Mewes, *J. Biol. Rhythms* **18**, 183 (2003).
 - [8] D. A. Golombek and R. E. Rosenstein, *Physiol. Rev.* **90**, 1063 (2010).
 - [9] Y. Hasegawa and M. Arita, *J. R. Soc. Interface* **11**, 20131018 (2014).
 - [10] C. Troein, J. C. Locke, M. S. Turner, and A. J. Millar, *Curr. Biol.* **19**, 1961 (2009).
 - [11] C. Troein, F. Corellou, L. E. Dixon, G. van Ooijen, J. S. O'Neill, F.-Y. Bouget, and A. J. Millar, *Plant J.* **66**, 375 (2011).
 - [12] U. Albrecht, B. Zheng, D. Larkin, Z. S. Sun, and C. C. Lee, *J. Biol. Rhythms* **16**, 100 (2001).
 - [13] S. Steinlechner, B. Jacobmeier, F. Scherbarth, H. Dernbach, F. Kruse, and U. Albrecht, *J. Biol. Rhythms* **17**, 202 (2002).
 - [14] R. Refinetti, *Circadian physiology* (Taylor & Francis, 2005), 2nd ed.
 - [15] W. J. Schwartz, M. Tavakoli-Nezhad, C. M. Lambert, D. R. Weaver, and H. O. de la Iglesia, *PNAS* **108**, 17219 (2011).
 - [16] Y. Kuramoto, *Chemical Oscillations, Waves, and Turbulence* (Dover publications, Mineola, New York, 2003).
 - [17] S. R. Taylor, R. Gunawan, L. R. Petzold, and F. J. Doyle III, *IEEE Trans. Automat. Contr.* **53**, 177 (2008).
 - [18] Y. Hasegawa and M. Arita, *J. R. Soc. Interface* **10**, 20121020 (2013).
 - [19] See Supplemental Material, which includes Ref. [20].
 - [20] R. Storn and K. Price, *J. Glob. Optim.* **11**, 341 (1997).
 - [21] A. Johnsson and W. Engelmann, in *Photobiology: The Science of Life and Light* (Springer, 2007).
 - [22] D. L. Hartmann, *Global Physical Climatology* (Academic Press, 1994).
 - [23] S. B. S. Khalsa, M. E. Jewett, C. Cajochen, and C. A. Czeisler, *J. Physiol.* **549**, 945 (2003).
 - [24] H. R. Ueda, W. Chen, A. Adachi, H. Wakamatsu, S. Hayashi, T. Takasugi, M. Nagano, K.-i. Nakahama, Y. Suzuki, S. Sugano, et al., *Nature* **418**, 534 (2002).

Supplemental Material for “Optimal Implementations for Reliable Circadian Clocks”

Yoshihiko Hasegawa and Masanori Arita

This supplemental material describes detailed calculations introduced in the main text. Equation and figure numbers in this section are prefixed with S (e.g., Eq. (S1) or Fig. S1). Numbers without the prefix (e.g., Eq. (1) or Fig. 1) refer to numbers in the main text.

1 Optimization

We calculated the optimal phase-response curves (PRCs) using two approaches, variational and numerical methods, whose explicit procedures are described below.

1.1 Variational method

Regularity \mathcal{V}_T and entrainability \mathcal{E} are calculated in our previous study [1]. Regularity is defined by the period variance of the oscillation (higher regularity corresponds to smaller period variance), which is represented by

$$\mathcal{V}_T = \frac{T^3}{4\pi^3} \int_0^{2\pi} \sum_{i=1}^N U_i(\theta)^2 Q_i(\theta)^2 d\theta. \quad (\text{S1})$$

Here N is the dimension, $U_i(\phi)$ is the infinitesimal PRC (iPRC), T is the period of the unperturbed oscillator and $Q_i(\phi)$ is a multiplicative noise term (see the main text). Entrainability, the extent of synchronization to a periodic input signal, is defined by the width of the Arnold tongue. Given a periodic input signal $p(\omega t)$ (ω is angular frequency), entrainability is represented by

$$\mathcal{E} = \Theta(\psi_M) - \Theta(\psi_m), \quad (\text{S2})$$

$$= \frac{1}{2\pi} \int_0^{2\pi} Z(\theta) \{p(\theta - \psi_M) - p(\theta - \psi_m)\} d\theta, \quad (\text{S3})$$

where $\Theta(\psi) = (2\pi)^{-1} \int_0^{2\pi} Z(\psi + \theta)p(\theta)d\theta$, $\psi_M = \operatorname{argmax}_\psi \Theta(\psi)$, $\psi_m = \operatorname{argmin}_\psi \Theta(\psi)$ and $Z(\phi)$ is the parametric PRC (pPRC) defined in Eq. (1).

The optimal PRCs, which maximize entrainability \mathcal{E} under constant regularity $\mathcal{V}_T = \sigma_T^2$, can be calculated by the Euler–Lagrange variational method. A variational equation to be optimized is

$$\mathcal{L} = \mathcal{E} - \lambda \mathcal{V}_T, \quad (\text{S4})$$

where λ is a Lagrange multiplier. With Eqs. (1), (S1) and (S3), Eq. (S4) is specifically given by

$$\mathcal{L} = \frac{1}{2\pi} \int_0^{2\pi} \sum_{i=1}^N \left\{ \{p(\theta - \psi_M) - p(\theta - \psi_m)\} U_i(\theta) \frac{\partial F_i(\theta; \rho)}{\partial \rho} - \frac{\lambda T^3}{2\pi^2} U_i(\theta)^2 Q_i(\theta)^2 \right\} d\theta, \quad (\text{S5})$$

where $F_i(\phi; \rho)$ is the i th reaction rate and ρ is a light-sensitive parameter. The functional derivative of \mathcal{L} with respect to U_i yields

$$\begin{aligned} \frac{\delta \mathcal{L}}{\delta U_i} &= \{p(\theta - \psi_M) - p(\theta - \psi_m)\} \frac{\partial F_i(\theta; \rho)}{\partial \rho} - \frac{\lambda T^3}{\pi^2} U_i(\theta) Q_i(\theta)^2, \\ &= 0. \end{aligned} \quad (\text{S6})$$

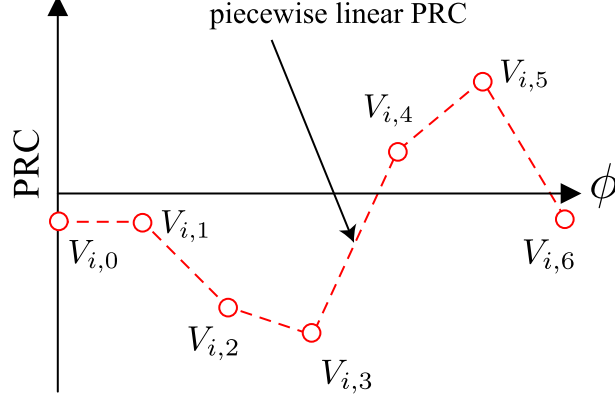


Figure S1: Piecewise linear PRC ($K = 6$) as an approximation of the iPRC $U_i(\phi)$, where the l th knot is $V_{i,l}$ (circle). We set $V_{i,K} = V_{i,0}$ for a periodic condition.

Solving Eq. (S6), we obtain the optimal PRCs $U_i(\phi)$ and $Z(\phi)$ given by

$$U_i(\phi) = \frac{\pi^2}{T^3 \lambda} \frac{p(\phi - \psi_M) - p(\phi - \psi_m)}{Q_i(\phi)^2} \frac{\partial F_i(\phi; \rho)}{\partial \rho}, \quad (\text{S7})$$

$$Z(\phi) = \frac{\pi^2}{T^3 \lambda} \sum_{i=1}^N \frac{p(\phi - \psi_M) - p(\phi - \psi_m)}{Q_i(\phi)^2} \left(\frac{\partial F_i(\phi; \rho)}{\partial \rho} \right)^2, \quad (\text{S8})$$

where the Lagrange multiplier λ is

$$\lambda = \sqrt{\frac{\pi}{4T^3 \sigma_T^2} \int_0^{2\pi} \sum_{i=1}^N \frac{[p(\theta - \psi_M) - p(\theta - \psi_m)]^2}{Q_i(\theta)^2} \left(\frac{\partial F_i(\theta; \rho)}{\partial \rho} \right)^2 d\theta}. \quad (\text{S9})$$

A substitution of Eq. (S8) into Eq. (S3) yields the entrainability \mathcal{E} represented by

$$\begin{aligned} \mathcal{E} &= \frac{1}{2\pi} \int_0^{2\pi} \{p(\theta - \psi_M) - p(\theta - \psi_m)\} \sum_{i=1}^N U_i(\theta) \frac{\partial F_i(\theta; \rho)}{\partial \rho} d\theta, \\ &= \frac{\pi}{2T^3 \lambda} \int_0^{2\pi} \sum_{i=1}^N \frac{\{p(\theta - \psi_M) - p(\theta - \psi_m)\}^2}{Q_i(\theta)^2} \left(\frac{\partial F_i(\theta; \rho)}{\partial \rho} \right)^2 d\theta. \end{aligned} \quad (\text{S10})$$

We maximize \mathcal{E} as functions of Δ and δ , where $\Delta = \psi_M - \psi_m$ and $\delta = \psi_m$. Substituting the obtained parameters into Eqs. (S7) and (S8), we can calculate the optimal PRCs [1].

The dead zone length L is defined by the length of null parts in the PRCs. Because a dead zone emerges when $\Delta \neq \pi$ in Eqs. (S7) and (S8), we can naturally define its length by

$$L = |\Delta - \pi|, \quad (\text{S11})$$

which is plotted in Fig. 2(b) as a function of the phase difference ν .

1.2 Numerical method

Because the optimal iPRC $U_i(\phi)$ and parameters (ψ_M and ψ_m) are interdependent, the variational method is not trivial. Consequently, to verify the correctness of the variational method numerically, we calculated the optimal PRCs with the evolutionary algorithm (specifically, we used a differential evolution (DE) of Storn and Price [2] provided by *MATHEMATICA* 9). Dividing the iPRC $U_i(\phi)$ into a piecewise linear function, we can reduce the variational problem to a conventional multivariate parameter optimization problem. We divide the iPRC $U_i(\phi)$ into K regions (Fig. S1) and linearly connect each knot to create a piecewise linear function as an approximation to U_i , where the value of the l th knot is given by $V_{i,l}$ for $l = 0, 1, \dots, K - 1$ (we set $V_{i,K} = V_{i,0}$ for a periodic condition):

$$U_i(\phi) \simeq \text{LF}(\phi; \mathbf{V}_i).$$

Here $\text{LF}(\phi; \mathbf{V}_i)$ is a piecewise linear function (LF is short for linear function) whose knots are $\mathbf{V}_i = (V_{i,0}, V_{i,1}, \dots, V_{i,K-1})$. Based on Eq. (4) in the main text, we let $U_{j_i}(\phi)$ be the iPRC of molecular species that have an i th light entry point (for the M input case there are M iPRCs $U_{j_1}(\phi), \dots, U_{j_M}(\phi)$). The constraint on the period variance is taken into account by considering scaled knots $\kappa \mathbf{V}_i = (\kappa V_{i,0}, \dots, \kappa V_{i,K-1})$ where κ is a scaling parameter determined by the variance constraint (κ is determined so that a piecewise linear PRC with $\kappa V_{i,0}, \kappa V_{i,1}, \dots, \kappa V_{i,K-1}$ yields the period variance $\mathcal{V}_T = \sigma_T^2 = 1$). The period variance (Eq. (S1)) for $\text{LF}(\phi; \kappa \mathbf{V}_{j_i})$ is given by

$$\sigma_T^2 = \frac{T^3}{4\pi^3} \int_0^{2\pi} \sum_{i=1}^M \text{LF}(\theta; \kappa \mathbf{V}_{j_i})^2 Q_{j_i}(\theta)^2 d\theta = \frac{\kappa^2 T^3}{4\pi^3} \int_0^{2\pi} \sum_{i=1}^M \text{LF}(\theta; \mathbf{V}_{j_i})^2 Q_{j_i}(\theta)^2 d\theta. \quad (\text{S12})$$

We adopted the assumption that the noise term $Q_i(\phi)$ is only present in input molecules $i = j_1, j_2, \dots, j_M$. Therefore, κ yielding the desired period variance σ_T^2 is calculated as

$$\kappa = \sqrt{\frac{4\pi^3 \sigma_T^2}{T^3 \int_0^{2\pi} \sum_{i=1}^M \text{LF}(\theta; \mathbf{V}_{j_i})^2 Q_{j_i}(\theta)^2 d\theta}}. \quad (\text{S13})$$

Because $\text{LF}(\phi; \mathbf{V}_i)$ is a linear function, the integral in Eq. (S13) can be calculated in a closed form.

We can calculate the entrainability \mathcal{E} with respect to the piecewise linear functions. We first calculate $\Theta(\psi)$ for $\text{LF}(\phi; \mathbf{V}_i)$ (again the integral can be calculated in a closed form):

$$\begin{aligned} \Theta(\psi; \mathbf{V}_{j_1}, \dots, \mathbf{V}_{j_M}) &= \frac{1}{2\pi} \int_0^{2\pi} p(\theta - \psi) \sum_{i=1}^M \text{LF}(\theta; \kappa \mathbf{V}_{j_i}) \frac{\partial F_{j_i}(\theta; \rho)}{\partial \rho} d\theta, \\ &= \frac{\kappa}{2\pi} \int_0^{2\pi} p(\theta - \psi) \sum_{i=1}^M \text{LF}(\theta; \mathbf{V}_{j_i}) \frac{\partial F_{j_i}(\theta; \rho)}{\partial \rho} d\theta. \end{aligned} \quad (\text{S14})$$

From Eq. (S2), the entrainability is given by

$$\mathcal{E}(\Delta, \delta, \mathbf{V}_{j_1}, \dots, \mathbf{V}_{j_M}) = \Theta(\Delta + \delta; \mathbf{V}_{j_1}, \dots, \mathbf{V}_{j_M}) - \Theta(\delta; \mathbf{V}_{j_1}, \dots, \mathbf{V}_{j_M}),$$

which is a function of $\Delta = \psi_M - \psi_m$, $\delta = \psi_m$ and $\mathbf{V}_{j_1}, \dots, \mathbf{V}_{j_M}$ ($\mathbf{V}_i \in \mathbb{R}^K$). For M iPRCs (M input pathways), $M \times K + 2$ parameters have to be optimized. The pPRC is calculated by Eq. (1):

$$Z(\phi) \simeq \sum_{i=1}^M \text{LF}(\phi; \kappa \mathbf{V}_{j_i}) \frac{\partial F_{j_i}(\phi; \rho)}{\partial \rho}, \quad (\text{S15})$$

$$Z_{j_i}(\phi) \simeq \text{LF}(\phi; \kappa \mathbf{V}_{j_i}) \frac{\partial F_{j_i}(\phi; \rho)}{\partial \rho}. \quad (\text{S16})$$

Z_{j_1} and Z_{j_2} by the evolutionary algorithm with $K = 20$ are plotted in Figs. 3(a) and (b) with circles and triangles, respectively (dashed and dot-dashed lines reflect the variational method).

2 Period dependence on constant light intensity

Under a constant light condition, the period may vary, depending on the light intensity. When a parameter ρ is perturbed $\rho + d\rho$ with $d\rho = \chi p(t)$ (for the constant light condition, $p(t) = 1$), the phase $\phi \in [0, 2\pi)$ obeys the following differential equation

$$\frac{d\phi}{dt} = \Omega + \chi Z(\phi) p(t), \quad (\text{S17})$$

where $\Omega = 2\pi/T$ is angular frequency of the oscillator and χ is the signal strength. In order to discuss a solution, we employ a perturbation expansion method. For the first order expansion, we assume that the solution $\phi(t)$ can be represented by

$$\phi(t) = \phi_0(t) + \chi \phi_1(t), \quad (\text{S18})$$

where $\phi_0(t)$ and $\phi_1(t)$ are zeroth- and first-order terms, respectively. Substituting Eq. (S18) into Eq. (S17) to obtain

$$\begin{aligned}\frac{d\phi_0}{dt} + \chi \frac{d\phi_1}{dt} &= \Omega + \chi Z(\phi_0 + \chi\phi_1)p(t), \\ &\simeq \Omega + \chi \{Z(\phi_0) + \chi\phi_1 Z'(\phi_0)\} p(t),\end{aligned}\tag{S19}$$

where we used $Z(\phi_0 + \chi\phi_1) \simeq Z(\phi_0) + \chi\phi_1 Z'(\phi_0)$. Equating Eq. (S19) with respect to the order of χ , we have the following coupled differential equations:

$$O(1) \quad \frac{d\phi_0}{dt} = \Omega,\tag{S20}$$

$$O(\chi) \quad \frac{d\phi_1}{dt} = Z(\phi_0)p(t).\tag{S21}$$

Integrating Eqs. (S20) and (S21) from $t = 0$ to $t = t_e$, where t_e is sufficiently large time, with an initial condition $\phi(0) = 0$, we have the following formal solutions:

$$\phi_0(t) = \Omega t,\tag{S22}$$

$$\phi_1(t_e) = \int_0^{t_e} Z(\Omega t)p(t)dt.\tag{S23}$$

From Eqs. (S18), (S22) and (S23), the phase ϕ at time $t_e = T$ with the input strength χ is given by

$$\begin{aligned}\phi(T; \chi) &= \phi_0(T) + \chi\phi_1(T), \\ &= 2\pi + \frac{\chi T}{2\pi} \int_0^{2\pi} Z(\theta)d\theta,\end{aligned}\tag{S24}$$

where we used $p(t) = 1$. For weak χ , the period T_χ , which is the period under the constant light condition with intensity χ , is approximated by

$$\frac{T_\chi}{T} \simeq \frac{\phi(T; 0)}{\phi(T; \chi)} = \frac{2\pi}{\phi(T; \chi)}.\tag{S25}$$

Substituting Eq. (S24) into Eq. (S25), we have

$$\begin{aligned}\frac{T_\chi}{T} &\simeq \frac{1}{1 + \frac{\chi T}{4\pi^2} \int_0^{2\pi} Z(\theta)d\theta}, \\ &\simeq 1 - \frac{\chi T}{4\pi^2} \int_0^{2\pi} Z(\theta)d\theta,\end{aligned}\tag{S26}$$

which is an equation shown in the main text.

3 Inference of intrinsic pPRC

pPRCs discussed in the main text are the intrinsic pPRCs, which govern internal phase dynamics of clocks. To observe the intrinsic pPRCs experimentally, short light pulses are applied to organisms to measure the phase shift induced by the pulses. Here we study a relation between intrinsic and observed pPRCs. We assume that a parameter ρ in clocks is perturbed $\rho + d\rho$ with $d\rho = \chi p(t)$ where the phase $\phi \in [0, 2\pi)$ obeys the same equation as Eq. (S17). Thus we use results of the perturbation expansion represented by Eqs. (S20) and (S21). For an input signal $p(t)$, we employed the squared pulse defined by

$$p(t; t_s) = \frac{1}{\ell} H(t - t_s) H(\ell + t_s - t),\tag{S27}$$

where $H(t)$ is the Heaviside step function defined by $H(t) = 1$ for $t \geq 0$ and $H(t) = 0$ for $t < 0$, t_s is onset time of the squared pulse and ℓ is the pulse duration (we express $p(t) = p(t; t_s)$ to represent explicit dependence on t_s). We plotted Eq. (S27) for two ℓ cases: $\ell = 1$ (solid line) and $\ell = 2$ (dashed line) in Fig. S2(a). With Eq. (S27), Eq. (S23) is specifically represented by

$$\phi_1(t_e) = \int_0^{t_e} Z(\Omega t)p(t; t_s)dt = \frac{1}{\ell} \int_{t_s}^{t_s + \ell} Z(\Omega t)dt.\tag{S28}$$

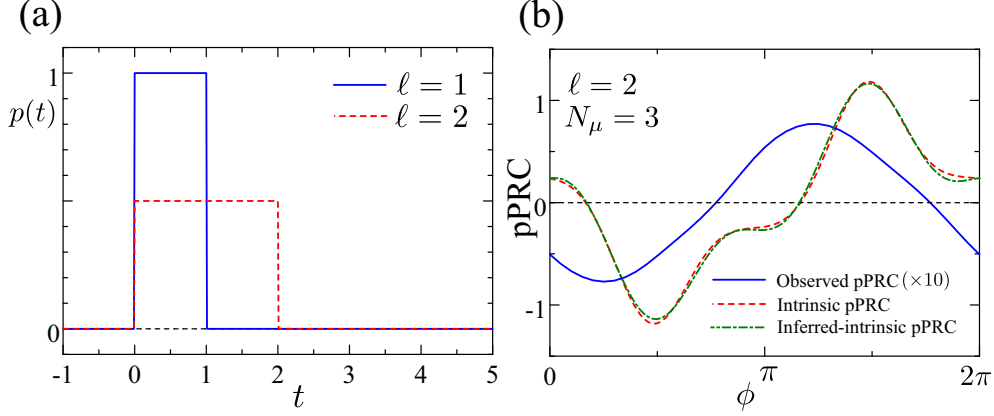


Figure S2: (a) Squared pulses $p(t; t_s = 0)$ with the duration $\ell = 1$ (solid line) and $\ell = 2$ (dashed line). (b) pPRCs of the oscillator model of Eqs. (S33)–(S34): observed pPRC (solid line; the magnitude is multiplied by 10) which is observed with $\ell = 2$ and $\chi = 0.1$, intrinsic pPRC (dashed line) and inferred intrinsic pPRC (dot-dashed line) by Eq. (S32).

Here we expand $Z(\phi)$ by the Fourier series up to N_μ th order

$$Z(\phi) = \sum_{\mu=-N_\mu}^{N_\mu} c_\mu \exp(i\mu\phi), \quad (\text{S29})$$

where c_μ is an expansion coefficient. Substituting Eq. (S29) into Eq. (S28), we have

$$\phi_1(t) = \sum_{\mu=-N_\mu}^{N_\mu} \frac{ic_\mu}{\ell\mu\Omega} \{1 - \exp(i\mu\Omega\ell)\} \exp(i\mu\Omega t_s).$$

Let $\tilde{Z}(\phi; \ell)$ be an observed pPRC by the squared pulse with the duration ℓ . Because the observed pPRC as a function of onset phase of the squared-pulse is quantified by the phase shift induced by the squared-pulse, the observed pPRC $\tilde{Z}(\phi; \ell)$ can be expressed by

$$\tilde{Z}(\phi; \ell) = \chi \sum_{\mu=-N_\mu}^{N_\mu} \frac{ic_\mu}{\ell\mu\Omega} \exp(i\mu\phi) \{1 - \exp(i\mu\Omega\ell)\}. \quad (\text{S30})$$

We also expand $\tilde{Z}(\phi; \ell)$ with respect to the Fourier series:

$$\tilde{Z}(\phi; \ell) = \sum_{\mu=-N_\mu}^{N_\mu} \tilde{c}_\mu \exp(i\mu\phi), \quad (\text{S31})$$

where \tilde{c}_μ is an expansion coefficient. Equating Eqs. (S30) and (S31), we can represent c_μ by

$$c_\mu = \begin{cases} -\frac{1}{\chi} \frac{i\tilde{c}_\mu \mu \Omega \ell}{1 - \exp(i\mu\Omega\ell)} & \mu \neq 0 \\ \frac{\tilde{c}_\mu}{\chi} & \mu = 0 \end{cases}, \quad (\text{S32})$$

which shows that the observed pPRC agrees with the intrinsic one (except for scaling) only when the squared pulse is the δ -peaked function ($\ell = 0$). For $\ell > 0$, it is impossible to completely restore the intrinsic pPRC from the observation, because higher order harmonics in the intrinsic pPRC are masked by the duration (μ th order harmonics where $|\mu|$ is sufficiently smaller than T/ℓ can be properly restored).

In order to check the reliability of the inference method, we applied to a simple oscillator model

$$\frac{dx}{dt} = x - x^3 - y + \rho, \quad (\text{S33})$$

$$\frac{dy}{dt} = x, \quad (\text{S34})$$

where ρ is a light sensitive parameter (Eq. (S33) corresponds to an additive case). The intrinsic pPRC of the oscillator is described by dashed line in Fig. S2(b). For test data, we artificially generated an observed pPRC which is the phase difference $\Delta\phi$ caused by the squared-pulse with the duration ℓ . We applied $\rho \rightarrow \rho + d\rho$ to Eq. (S33) where $\rho = 0$ and $d\rho = \chi p(t; t_s)$ ($\ell = 2$ and $\chi = 0.1$) and the phase difference $\Delta\phi$ as a function of onset phase of the pulse is used as the observed pPRC which is plotted in Fig. S2(b) (solid line; the magnitude is multiplied by 10). The dot-dashed line in Fig. S2(b) shows an inferred intrinsic pPRC through Eq. (S32) which is calculated with $N_\mu = 3$ order approximation (i.e. we approximated the observed pPRC with the third order Fourier series and applied Eq. (S32)). We see excellent agreement between the inferred (dot-dashed line) and true (dashed line) intrinsic pPRCs, which verifies the reliability of the inference method.

References

- [1] Y. Hasegawa and M. Arita. Circadian clocks optimally adapt to sunlight for reliable synchronization. *J. R. Soc. Interface*, 11:20131018, 2014.
- [2] R. Storn and K. Price. Differential evolution - a simple and efficient heuristic for global optimization over continuous spaces. *J. Glob. Optim.*, 11:341–359, 1997.